

Planetary transit candidates in the CoRoT initial run: resolving their nature^{★,★★}

C. Moutou¹, F. Pont², F. Bouchy³, M. Deleuil¹, J. M. Almenara⁴, R. Alonso¹, M. Barbieri¹, H. Bruntt⁵, H. J. Deeg⁴, M. Fridlund⁶, D. Gandolfi⁷, M. Gillon⁸, E. Guenther⁷, A. Hatzes⁷, G. Hébrard³, B. Loeillet¹, M. Mayor⁸, T. Mazeh⁹, D. Queloz⁸, M. Rabus⁴, D. Rouan⁵, A. Shporer⁹, S. Udry⁸, S. Aigrain², M. Auvergne⁵, A. Baglin⁵, P. Barge¹, W. Benz¹⁰, P. Bordé¹¹, S. Carpano⁶, R. De la Reza¹², R. Dvorak¹³, A. Erikson¹⁴, P. Gondoin⁶, T. Guillot¹⁵, L. Jorda¹, P. Kabath¹⁴, H. Lammer¹⁶, A. Léger¹¹, A. Llebaria¹, C. Lovis⁸, P. Magain¹⁷, M. Ollivier¹¹, M. Pätzold¹⁸, F. Pepe⁸, H. Rauer¹⁴, J. Schneider¹⁹, and G. Wuchter⁷

¹ Laboratoire d'Astrophysique de Marseille, 38 rue Frédéric Joliot-Curie, 13388 Marseille Cedex 13, France
e-mail: Claire.Moutou@oamp.fr

² School of Physics, University of Exeter, Exeter, EX4 4QL, UK

³ IAP, 98bis boulevard Arago, 75014 Paris, France

⁴ Instituto de Astrofísica de Canarias, 38205 La Laguna, Tenerife, Spain

⁵ LESIA, Obs de Paris, Place J. Janssen, 92195 Meudon Cedex, France

⁶ Research and Scientific Support Department, ESTEC/ESA, PO Box 299, 2200 AG Noordwijk, The Netherlands

⁷ Thüringer Landessternwarte, Sternwarte 5, Tautenburg 5, 07778 Tautenburg, Germany

⁸ Observatoire de l'Université de Genève, 51 chemin des Maillettes, 1290 Sauverny, Switzerland

⁹ School of Physics and Astronomy, Raymond and Beverly Sackler Faculty of Exact Sciences, Tel Aviv University, Tel Aviv, Israel
¹⁰ Bern, Switzerland

¹¹ Institut d'Astrophysique Spatiale, Université Paris XI, 91405 Orsay, France

¹² Observatório Nacional, Rio de Janeiro, RJ, Brazil

¹³ University of Vienna, Institute of Astronomy, Türkenschanzstr. 17, 1180 Vienna, Austria

¹⁴ Institute of Planetary Research, German Aerospace Center, Rutherfordstrasse 2, 12489 Berlin, Germany

¹⁵ Observatoire de la Côte d'Azur, Laboratoire Cassiopée, BP 4229, 06304 Nice Cedex 4, France

¹⁶ Space Research Institute, Austrian Academy of Science, Schmiedlstr. 6, 8042 Graz, Austria

¹⁷ University of Liège, Allée du 6 août 17, Sart Tilman, Liège 1, Belgium

¹⁸ Rheinisches Institut für Umweltforschung an der Universität zu Köln, Aachener Strasse 209, 50931, Germany

¹⁹ LUTH, Observatoire de Paris, CNRS, Université Paris Diderot, 5 place Jules Janssen, 92195 Meudon, France

Received 20 February 2009 / Accepted 4 May 2009

ABSTRACT

With the release of CoRoT lightcurves of the Initial Run IRa01, 50 transiting planetary candidates have been published in a companion paper. About twenty of them were identified as binary stars from the CoRoT lightcurve itself. Complementary observations were conducted for 29 candidates, including ground-based photometry and radial-velocity measurements. Two giant planets were identified and fully characterized. Nineteen binaries are recognized, from which 10 are background eclipsing binaries in the CoRoT mask or triple systems, diluted by the main CoRoT target. Eight cases remain of unclear origin, one of them still being a planetary candidate. Comparison with simulations shows that the actual threshold of confirmed planet detection in this field does not yet fulfill the expectations, and a number of reasons are invoked, like the ranking process based on lightcurve analyses, and the strategy and limits of follow-up observations for targets fainter than magnitude 15.

Key words. stars: planetary systems – techniques: photometric – techniques: radial velocities – techniques: spectroscopic

1. Introduction

Compared to ground-based transit surveys, space-based stellar photometry with CoRoT allows the detection of new classes

of transiting planets, characterized by a small radius or a long orbital period. This, however, requires an extensive effort of complementary observations, consisting of ground-based photometry, spectroscopy, and high-precision radial-velocity measurements. This paper presents the analysis of transit candidates detected in the Initial Run of CoRoT, IRa01, obtained by the CoRoT exoplanet science team after two years of complementary observations. The Initial Run took place from JD = 2 454 138 to 2 454 193 (6 February to 2 April 2007) for a total duration of 55 days. This study is a companion paper to the one presenting the detections themselves (Carpano et al. 2009, hereafter Paper I), with the aim of identifying the best

* Based on data obtained at Observatoire de Haute Provence with SOPHIE and with HARPS on the ESO 3.6 m telescope at La Silla Observatory. The CoRoT space mission, launched on December 27th 2006, has been developed and is operated by CNES, with the contribution of Austria, Belgium, Brazil, ESA (RSSD and Science Programme), Germany and Spain.

** Tables 2 to 13, 15 to 17 and Figs. 4 to 7 are only available in electronic form at <http://www.aanda.org>

scenario and explaining the signal seen by CoRoT, when possible. Paper I presents fifty detected planetary candidates and 141 eclipsing binaries from a total of 9872 targets observed during IRa01. Complementary observations were performed on the 29 most promising planetary candidates. Their folded lightcurve is shown in Figs. 4 to 7 in electronic form.

The instruments and methods used for the complementary observations are listed in Table 1, including the CCD imaging cameras, and spectrographs. Pre-launch observations of the IRa01 targets were performed in 2002–2005, aiming at measuring the magnitudes, colors and positions prior to the launch building the exoplanet entry catalog EXODAT (Deleuil et al. 2009). This information is reported in Table 2. First estimates on the spectral classification of the parent stars were obtained by isochrone fitting of multi-color optical and near-infrared photometry (Barbieri et al., in prep.). After the detection of transit candidates, a classical strategy of follow-up observations was applied, in order to check whether the main target is responsible for the CoRoT transit -or rather, some nearby star included in the photometric mask integrated onboard-, and if the mass ratio between the parent star and the transiting body is small enough to exclude an eclipsing binary. Most difficult to reject are the triple systems or diluted eclipsing binaries within a typical one arcsec radius. For a description of scenarios that mimic a planetary transit and conventional strategies to discard them, see for instance Brown (2003) and Bouchy et al. (2009).

In the following, we will describe case by case all follow-up observations realized in the context of the IRa01 transiting candidate identification. Not all events described in Paper I required complementary observations. For 20 of them, a binary origin was proposed from the lightcurve analysis itself, or the candidates were not convincing enough. We refer to Paper I for all transit parameters. CoRoT targets and transit candidates are identified with a unique ID (e.g. 0102723949) and a run ID (e.g. IRa01-E1-2046). We will use both identifiers in the tables, figures and section names, but only the shortcut of the run ID (e.g. E1-2046) in the text. CoRoT data of IRa01 are accessible at the URL: <http://idc-corotn2-public.ias.u-psud.fr/> and EXODAT stellar data are available at: <http://lamwvs.oamp.fr/exodatpub>

2. Resolution of transit candidates

2.1. Planets

E2-1126/0102890318/CoRoT-1b

The transits of E2-1126 were detected by the alarm mode (Surace et al. 2008), during the CoRoT operations on the initial run. The observations conducted on SOPHIE quickly established the planetary nature of the transiting body, that was then called CoRoT-1b (Barge et al. 2008). The transiting planet is a giant gaseous planet with a $1.49 R_{\text{Jup}}$ radius. The radial-velocity (RV) observations were continued 6 months after this early discovery. We have now gathered 52 measurements with both SOPHIE and HARPS spectrographs, which show no significant variation compared to earlier analyses, neither in terms of long-term drift nor non-zero eccentricity (Pont et al., in prep.). In addition, the transit has been observed by HARPS, and by VLT/FORS2 in *B* and *V* filters, to constrain its shape. A better characterisation of the stellar parameters is ongoing from the sequence of HARPS spectra, and especially, the very low metallicity of the parent star is under revision. In-depth analyses of new complementary data on CoRoT-1 will be published in forthcoming papers

(Pont et al., in prep.; Deleuil et al., in prep.; Gillon et al., 2009), while some recent analyses of the CoRoT-1 lightcurve have been published (Bean 2009; Snellen et al. 2009; Alonso et al. 2009).

E1-0330/0102912369/CoRoT-4b

The candidate E1-0330, with 1.2% deep transits and a 9.202 day period, has been established as of planetary origin by SOPHIE in October 2007. The data are presented and discussed by Aigrain et al. (2008) and Moutou et al. (2008). The planet has a mass of $0.72 M_{\text{Jup}}$ and a radius of $1.19 R_{\text{Jup}}$, and orbits an FOV star with a rotation period similar to the giant planet's orbital period. Six new HARPS measurements were obtained one year after the earlier announcement. These new data do not change the orbital solution nor indicate a second planet in the system.

2.2. Eclipsing binaries as the main target

E1-2046/102723949

The candidate E1-2046 shows a 1.17% deep single transit in IRa01 at JD = 2454 167.91. Given the total duration of the time series (55 days), this implies that the orbital period is larger than 33 days. It turns out that the same star was also observed during the CoRoT run LRa01, one year later, and that its period is 50.2 days. One SOPHIE spectrum was acquired on 29 February 2008. The cross-correlation function indicates a spectroscopic binary of type 2 (SB2), with two components separated by 31 km s^{-1} (Fig. 1). One exposure was thus sufficient to discard this single-transit candidate as an eclipsing binary. We did not try to constrain the secondary mass with a second measurement, nor to check whether the velocity variation was in phase with the CoRoT ephemeris.

E2-3010/102800106

CoRoT measured a long period (23.2 days), deep (1.72%) transit for E2-3010. We performed one HARPS observation on 13 January 2008, at phase = 0.81. We obtained the cross-correlation function of an SB2 system. The two peak velocities are separated by 23.2 km s^{-1} (Fig. 1). One component is wide (22 km s^{-1}) and one is narrow (6.6 km s^{-1}), implying different projected rotational velocities. Although we cannot guarantee that there is no planet in this system, confirming it and characterizing its mass would require too large an effort in RV observations. We therefore reject such systems.

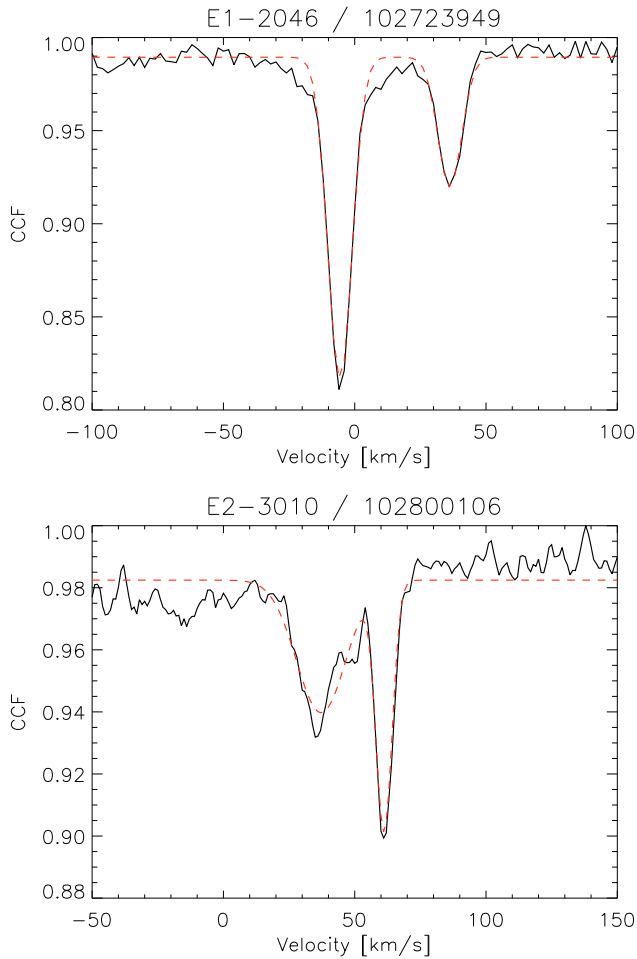
E2-3854/102841669

With a very short period (1.14 day) and a very shallow (0.136%) transit signal, the CoRoT lightcurve of candidate E2-3854 seemed very promising. Two SOPHIE observations were made on 28 January and 8 February 2008 (Table 3). The cross-correlation function shows two peaks separated by about 80 km s^{-1} , which allows us to reject this candidate as an eclipsing binary. With two exposures and the CoRoT ephemeris, we are able to estimate the orbital solution for this system, assuming circular orbits (Fig. 2). The mass ratio of the system is about 1. Although the primary star is classified as a giant star by pre-launch analysis, the short orbital period refutes this possibility, as the orbital distance of the secondary would have to be smaller than the primary radius; this illustrates how photometric classification can lead to incorrect estimates (see Sect. 3.1).

Table 1. Instruments and methods used in the complementary observations of the IRa01 candidates.

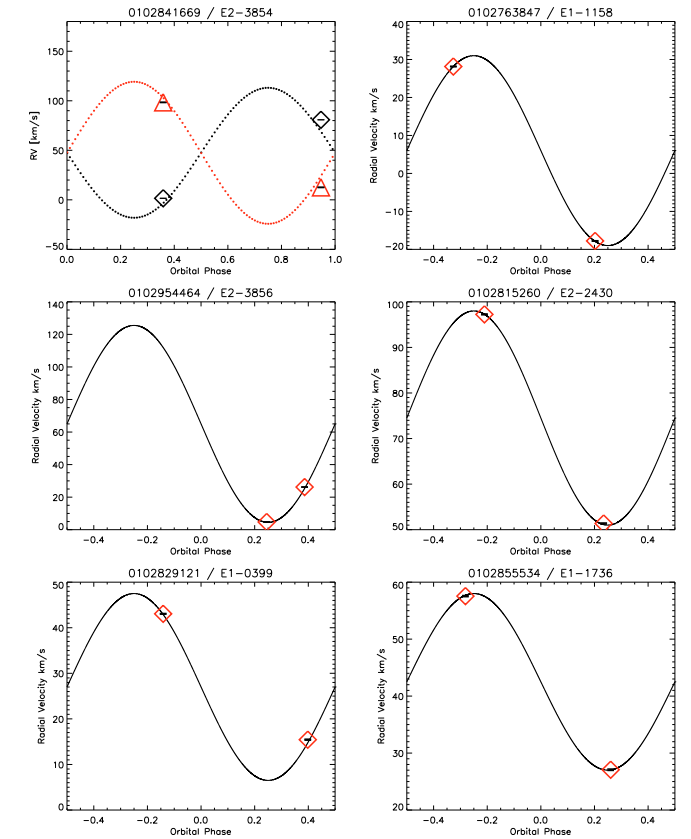
Instrument	Diam Tel	Nb Nights ^a	Method	Measurement ^b
INT/WFC	2.5	5	photometry	pre-launch spectral typing, astrometry
IAC80	0.8	0.5	photometry	on-target transit confirmation
EulerCam	1.2	3	photometry	on-target transit confirmation
Wise/0.46	0.46	3	photometry	on-target transit confirmation
Wise/1.0	1.0	3	photometry	on-target transit confirmation
CFHT/Megacam	3.6	1.5	photometry	on-target transit confirmation
CORALIE	1.2	1	radial velocity	SB identification
SOPHIE	1.93	7	radial velocity	SB identification, mass characterization
HARPS	3.6	5	radial velocity	SB identification, stellar parameters mass characterization
UVES	8.0	0.5	spectroscopy	stellar parameters

^a The approximate number of nights per instrument is given as an indication of the observational effort needed for the follow-up of a single CoRoT field. ^b SB stands for spectroscopic binary.

**Fig. 1.** Cross-correlation functions of two SB2 in the sample, E1-2046 and E2-3010. Dotted lines are Gaussian fits to the data.

E1-1158/102763847

We followed the candidate E1-1158 (transit depth 1.36% and orbital period 10.53 days), with the spectrograph SOPHIE on 24 and 29 February 2008 (Table 4). The star is a fast rotator, with $v \sin i \simeq 18 \text{ km s}^{-1}$. Photometry indicates an F-type star with $1.5 M_{\odot}$. The velocities obtained near the expected extrema are separated by 46 km s^{-1} , hence the system is a spectroscopic

**Fig. 2.** Radial-velocity curve and rough adjustment of an orbital solution, for one SB2 and 5 SB1 found in our sample.

binary of type 1 (SB1). The semi-amplitude of the orbit, if circular, is 25 km s^{-1} , and the mass ratio is 0.22 (Fig. 2).

E1-0399/102829121

The lightcurve of the candidate E1-0399 shows a 1.5% deep transit every 33.06 days. The target was observed by CORALIE on 12 and 30 January 2008. The velocities measured at phases 0.86 and 0.39 are separated by 27 km s^{-1} , indicating an SB1 system. When the data are fitted with a circular orbit, one gets a semi-amplitude of 20.5 km s^{-1} and a mass ratio of 0.31.

E2-3856/102954464

Despite the long orbital period (16.56 days), the star was observed with the Swiss 1.2 m Euler telescope at La Silla for on-off photometry. During an on-transit night in April 2008, an eclipse of about 2% depth was detected on the main target, at the CoRoT predicted ephemeris. The depth is also comparable to the one measured by CoRoT. The star was also observed by HARPS, on 5 March and 24 March 2008. The RV measurements show a single cross-correlation peak, separated by more than 20 km s^{-1} from the first night to the second (Table 6), while only sampling a small fraction of the orbit. Under the assumptions that the spectroscopic binary follows the CoRoT ephemeris (since it is transiting), and that the orbit is circular, it would correspond to a semi-amplitude K of about 60 km s^{-1} (Fig. 6). The mass ratio between both components of the stellar system would then be 0.7.

E2-0203/0102825481

The transit candidate E2-0203 was identified by the alarm mode, in March 2007, when the CoRoT observations of the IRa01 field were still ongoing. The transits are of 3.4% depth and with a period of 5.168 days. Ground-based photometry with the IAC 80 cm (30 March 2007) telescope and Canada-France-Hawaii telescope (10 April 2007) confirmed the eclipse occurring on the main star of the CoRoT photometric aperture. The spectroscopic observations started on 26 March 2007 at Tautenburg observatory, and were continued until 18 April. The star is a spectroscopic binary at the period and phase determined by CoRoT. The RV semi-amplitude inferred from the observations is 16.9 km s^{-1} . The primary star is of slightly later type than the Sun, and the secondary is a low-mass M star. With a mass ratio of 0.142 and radius ratio 0.184, this secondary belongs to the rare population of very low-mass stars. The refined analysis of the complete lightcurve shows the detection of the secondary eclipse, 40 times shallower than the primary transit; it is detected with 11σ significance at phase 0.514, as expected for a slightly eccentric orbit (Fig. 4). An in-depth analysis of E2-0203, including a discussion of the secondary transit, the orbital eccentricity, and additional measurements, will be presented in an article by Morales et al. (in prep.).

E2-2430/102815260

CoRoT observations of E2-2430 have revealed a transit event of 1.16% depth and 3.587 day orbital period. SOPHIE observations of E2-2430 were conducted on February 5 and 7, 2008, near the expected RV extrema (Table 7). The measurements are separated by 46 km s^{-1} . The parent star is a fast-rotating F-type star (projected velocity of 30 km s^{-1}), indicated by a wide cross-correlation function and few absorption lines in the optical spectrum. This system is an SB1, with a semi-amplitude of 23.5 km s^{-1} and mass ratio of about 0.17 (Fig. 2).

E2-1736/102855534

We acquired two SOPHIE observations of E2-1736 (1.18% deep transit at period 21.72 days) on 31 January and 10 February 2008 (Table 8). The star is rotating rapidly, with a $v \sin i$ of 27 km s^{-1} , and the velocity difference is about 30 km s^{-1} between both expected extrema (Fig. 2). If the orbit is circular, which is questionable at the 21d period, then the RV semi-amplitude would be 15.5 km s^{-1} , corresponding to a mass ratio of 0.2. Further

analysis of the CoRoT lightcurve showed a faint secondary detected at $9\text{-}\sigma$ (Fig. 4).

Nine spectroscopic binaries were thus identified among the IRa01 transit candidates. It is noticeable that most of them have relatively low amplitudes of velocity variations, corresponding to small mass ratios, ranging from 0.14 to 0.3. This is explained by the fact that other types of binaries are easily rejected from the lightcurve analysis itself (Paper I). Only for extreme mass ratios is the secondary transit undetected in the high-precision and continuous CoRoT lightcurves. Along the same line, most of these binaries have long orbital periods, i.e. more than 10 days, for which no strong ellipsoidal variation is expected to appear in the lightcurve. This was expected from pre-launch simulations and is fully validated by the analysis of IRa01 candidates.

2.3. Background eclipsing binaries

The first cases presented in this section have been solved by photometry; they correspond to background eclipsing binaries (BEB) hidden within the wide photometric mask of CoRoT (typical size 20 arcsec). The other cases have been solved by spectroscopic observations. They usually correspond to blends with eclipsing binaries typically within the limits of ground-based seeing, ie 1 arcsec. Some have both photometric and RV evidence, allowing us to precisely describe the scenario, which is very likely related to physically associated triple systems.

E2-2604/102805893

Ground-based photometry with Euler in April 2008 was performed on this shallow (0.25%) transit, short period (3.82 days) candidate. On-off relative photometry showed no transit occurring on the main target. A nearby star, however, undergoes a 3% eclipse. The star is distant by 15 arcsec and 7.5 times brighter in R than the main target. With the known CoRoT PSF and the photometric aperture used, we estimated that about 1% of the flux of this background star pollutes the CoRoT mask (including distance and flux difference). Thus, the transit observed by CoRoT is caused by this background eclipsing binary.

E2-1136/102809071

The candidate E2-1136 also shows a short period transit signal with very shallow depth (0.17% and 1.224 day, respectively). On-off photometry performed both at Wise Observatory and with Euler found a nearby star with a 8% deep eclipse. The transit occurs on a stellar contaminant at 12 arcsec towards the east. Dilution from that star may explain the observed 0.17% deep Corot lightcurve. A deep analysis of the CoRoT lightcurve -not available at the time of follow-up operations- shows a secondary at opposite phase detected at a $8\text{-}\sigma$ level, further confirming the binary scenario (Fig. 4).

E2-4300/102802430

The lightcurve of E2-4300 shows a 0.5% deep transit occurring every 5.806 days. It was observed at a predicted transit time at Canada-France-Hawaii Telescope with Megacam on 10 January 2008. A nearby star at 10 arcsec towards the south-east and 0.95 mag fainter undergoes a 7% eclipse, at the expected epoch, while the main target has no photometric variation. The CoRoT transit is clearly caused by a BEB in the photometric mask.

E2-3425/102835817

The lightcurve of E2-3425 shows transits of 0.36% depth and 1.185 day period. The star was observed with HARPS in the high efficiency mode EGGs on 5 and 7 October 2008. The typical uncertainty on such a faint star with EGGs is of the order of 30 m/s. No variation is observed at this level between both measurements taken close to the expected RV extrema (Table 16). Ground-based photometry was performed on 31 January 2009 with Euler for this target, and shows that a star 1.2 times fainter than the main target and distant by 12 arcsec undergoes a 25% deep eclipse approximately at the predicted epoch. A shift of the central transit time of half an hour is observed, that is compatible with the measured ephemeris error and the gap between the CoRoT lightcurve and the Euler observation.

E1-0288/102787048

CoRoT detects a 0.37% deep transit with a 7.89 day orbital period in the lightcurve of E1-0288. Follow-up observations of E1-0288 started with ground-based photometry at the Observatoire de Haute Provence with the 120 cm telescope. Aperture photometry was performed on the seeing-limited images, and the conclusion was consistent with a transit occurring on the target star, at the expected CoRoT ephemeris. Radial velocity observations then started with SOPHIE; three measurements were done, from which no conclusions could be drawn (no RV variation). A second look at the OHP 120 cm data with DECPHOT (Gillon et al. 2007) then allowed us to separate the main target from a nearby star about 9 arcsec north and 1.3 magnitude fainter. When both stars can be separated, a 3% deep eclipse is detected on the faintest one. Once diluted in the flux of the main target, it well reproduces a 0.35% deep transit as seen by CoRoT. In parallel, we performed two measurements with HARPS on the nearby contaminant, and detected an SB1 with a semi-amplitude of 14.5 km s^{-1} (Bouchy et al. 2009), hence a mass ratio of 0.15. This is another low-mass stellar companion, with characteristics similar to E2-0203, as well as a BEB as suggested by the signal detected by CoRoT.

E2-0704/102855472

On-off photometry was performed with Euler on candidate E2-0704. However, these measurements were not obtained at an optimal orbital phase, and therefore the result is not conclusive. A nearby star located 11 arcsec to the south and five time fainter than the main target is a potential background eclipsing binary. HARPS observations obtained on 29 February and 1 March 2008 show no velocity variations between extreme phases (Table 9). It thus suggests that this eclipsing binary is in the background, within the CoRoT photometric mask, rather than the main target, although we do not have the ground-based confirmation of this scenario. Moreover, the secondary eclipse is unambiguously detected by CoRoT at the expected phase, and spectroscopic analysis of HARPS data shows that $T_{\text{eff}} \simeq 5400 \pm 200 \text{ K}$ and $\log g \simeq 3.0 \pm 0.5$; the main CoRoT target being a giant star, it is unlikely that it has a companion with a 2.15 day period, so the eclipsing binary detected by CoRoT has to be a nearby target.

E2-1857/102798247

The transit event of E2-1857 has 0.47% depth and an extremely short period of 0.822 days. SOPHIE observations of E2-1857 started in February 2008. We obtained

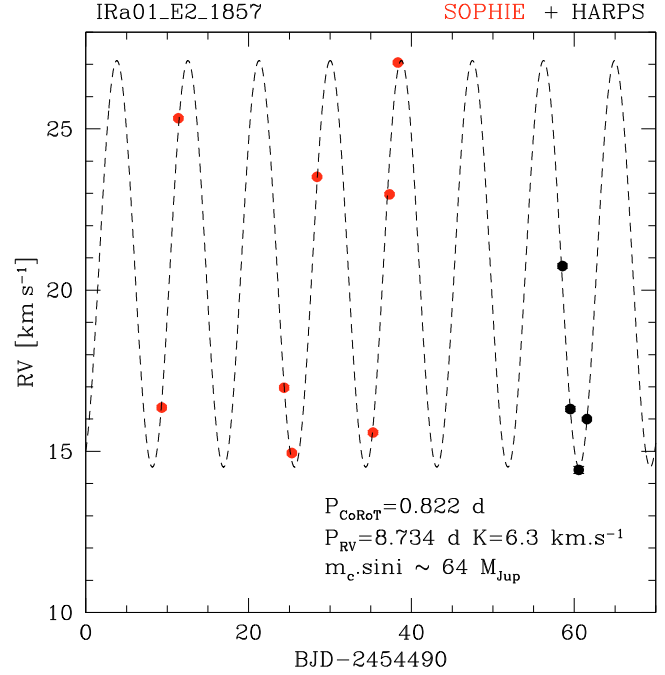


Fig. 3. The radial-velocity variation of E2-1857 as a function of time, including SOPHIE and HARPS variations. The superimposed orbit has a period of 8.734 days whereas the CoRoT period of 0.822 day is caused by a nearby background eclipsing binary.

8 measurements (Table 10), and measured a radial velocity fluctuation of a few km s^{-1} . A few measurements were also taken with HARPS in order to observe the bisector behaviour. With this data set, we found an orbital solution at a period of 8.734 days, whereas the CoRoT period is 0.822 day (Fig. 3). In parallel, on-off observations took place on Euler on 05 February 2008. After deconvolution photometry, an eclipsing nearby star is detected at 3 arcsec north-west of the main target, in phase with the CoRoT ephemeris. This star is 38 times fainter in R than the target. It undergoes a 11.5% drop in brightness during the expected transit while the target is stable. We thus observe both an eclipsing binary (a nearby faint star producing the CoRoT signal, diluted by the main target) and a spectroscopic binary (the main target). The eclipsing binary also shows a secondary eclipse at CoRoT phase 0.5, detected at the $10\text{-}\sigma$ level since then (Fig. 4). The primary target E2-1857 is a dwarf with an estimated effective temperature of 7200 K; its mass may be approximated as $1.6 M_{\odot}$. The semi-amplitude of the RV variations is 6.3 km s^{-1} at the 8.734 day period, which corresponds to a minimum mass of the companion of $0.1 M_{\odot}$. It is unlikely that two unrelated systems are seen edge-on within 3 arcsec from Earth, so that the real mass is probably significantly higher. The primary star E2-1857 is also classified as a δ Scuti variable.

E2-2009/102788073

In the lightcurve of E2-2009, CoRoT detected a transit of 0.41% depth occurring every 10.85 days. We gathered 7 SOPHIE spectra of E2-2009 between 6 February and 20 March 2008. With uncertainties ranging from 20 to 60 m/s, we could not detect significant RV variation at the CoRoT ephemeris. On 7 March 2008, Euler on-off photometric observations detected no variations, either on the main target or on the surrounding stars. This result could have indicated a potential small planet scenario, since the

CoRoT detected transit is rather shallow (0.004). We therefore performed two additional measurements with HARPS, with a greater accuracy than SOPHIE, on 22 and 25 March 2008, at phases 0.50 and 0.77. All RV measurements of E2-2009 are displayed in Table 11 and were presented by Bouchy et al. (2009) (see their Sect. 4.4 and Fig. 3). The difference between the measurements is from about 50 m/s to more than 200 m/s, depending on the numerical template spectrum that is used for the spectral cross-correlation (F0 to K5). Such a significant template dependence of the derived radial velocity is observed for triple systems, or binary systems blended with another stellar source. The largest velocity variation corresponds to the mask with closest spectral type to the primary star of the binary system, in this case, a K-type star. The bisector span also varies with the velocity, another signature of a diluted binary (Bouchy et al. 2009). Now, the RV variation should still be in phase with the CoRoT ephemeris to explain the detected photometric signal, which is not the case. The probable scenario is therefore a binary K system diluted by the CoRoT main target; having similar colours, it is not possible to distinguish primary and secondary transits of this system, while both are detected. The orbital period is then double the one measured by CoRoT, i.e. 21.691 days. Recalculating the phase, we now find a good agreement with the RV variation and the photometric signal (see Table 11). This scenario is also reinforced by 1) the observation of a slight asymmetry in the HARPS cross-correlation function, and a bisector effect; and 2) a V-shape transit, both findings suggesting a diluted grazing binary.

E1-2329/102869286

The candidate E1-2329 shows a transit of 0.37% depth and 1.876 day period in the CoRoT lightcurve. It was observed with HARPS on 22, 25 and 28 February 2008. The derived velocities are given in Table 12. As for E2-2009, we found a behaviour of the velocity that depends on the mask used for correlating the spectrum. In this case, no variation is observed with masks of K5 and G2 stars, while a 80 m/s velocity difference is seen when using the F0 mask (the error of HARPS observations is less than 20 m/s). This would mean an F-type primary of a binary system, blended by the CoRoT main target. The velocity variation is not consistent with the CoRoT ephemeris. If the period was double, however, the velocity would fit the expected behaviour. Thus this system, most probably, is a triple system with two eclipsing stars of the same colour, hotter than the Sun, and with an orbital period of 3.734 days.

E1-3336/102876631

The CoRoT transits of E1-3336 are 0.17% in depth, with a period of 1.389 day. Three SOPHIE spectra of E1-3336 were obtained early in February 2008. We could derive a low-amplitude RV variation in phase with CoRoT, and we continued the observation with HARPS to obtain higher accuracy. The 3 additional data points obtained with HARPS showed a different behaviour when using different cross-correlation masks (Table 13 and Fig. 3 in Bouchy et al. 2009). The highest RV amplitude is found for the F0 mask, implying an early-type primary star in a blended binary system. The velocity variation of the blended binary is in phase with the CoRoT ephemeris; the diluted eclipses of this double star are thus the origin of the photometric signal.

2.4. Unsolved cases

This section deals with stars for which spectroscopy revealed a fast rotating star or a hot star. Radial velocity measurements are impossible, or very limited in precision.

E1-0783/102895957

E1-0783 is a target with a single 0.64% transit in the full 58 day lightcurve, occurring 25 days after the initial epoch. Although the period is not measured, and ground-based photometric confirmation is impossible, the candidate is potentially of great interest for periods longer than 32 days. SOPHIE observed E1-0783 on 26 October 2008 and no cross-correlation function could be detected. The star is of early type with an effective temperature of about 7500 K, and a projected velocity higher than 350 km s^{-1} to blur the lines. Spectroscopy will not provide clues of possible grazing binaries. The transit depth marginally allows a secondary of planetary radius if the transit occurs on the main target: with a stellar radius of 1.4 to $3.0 R_{\odot}$, the transiting body has a radius larger than $1.1 R_{\text{Jup}}$.

E1-4617/102753331

The transit of E1-4617 is rather deep (4%) and of long period (19.76 days). In order to confirm or reject the planet hypothesis, HARPS observed this target on 19 February 2008, and could not detect a cross-correlation function. In the spectrum, only hydrogen Balmer lines and interstellar NaI doublet are visible. The star is of spectral type A, and radial velocity measurements are not possible. With a stellar radius greater than 2 solar radii, the 4% deep transit is however of stellar origin, rather than planetary. Pre-launch photometry indicates a main-sequence G star (Table 2), but degeneracy with a reddened early-type star is expected, even if requiring a relatively extreme colour excess of 0.6 mag, and we are more confident of spectroscopy for this rough spectral typing.

E2-4467/102940315

The 16.45 day period transit candidate E2-4467 (1.4% depth) was observed with HARPS on 27 February 2008. No cross-correlation function is detected and the spectrum shows only Balmer lines. This case is similar to E1-4617: the depth of the transit (1.4%) and the early-type primary makes a planetary origin impossible for the transit.

E1-4591/102806520

CoRoT detects 0.29% deep transits with a period 4.29 days in E1-4591. We obtained one HARPS spectrum of this target on 2 March 2008. With one hour exposure and a signal-to-noise ratio of about 20 at 550 nm, we have detected a very weak and wide cross-correlation function, characterized by a contrast of about 1% and a width of 21 km s^{-1} . This width corresponds to a projected velocity of about 16.4 km s^{-1} . The primary star is a modestly rotating F star. A second measurement was planned but never performed, because of the very low contrast of the cross-correlation function which prevents high-precision velocity measurements. If the rotation period of the star was the same as the orbital period, as in a synchronised binary system, it would lead to a $1.38 R_{\odot}$ primary star, and a secondary of $0.7 R_{\text{Jup}}$. This suggests a companion in the stellar mass range, able to trigger tidal synchronisation. Additionally, the lightcurve of

this target shows δ -Scuti-type periodic pulsations at a frequency of 11.8741 cycles/day (Fig. 4); strangely, the transit period is exactly 51 times the pulsation period, but such a large factor could be coincidence, rather than a signature of tidal interactions.

E2-1712/102826302

The candidate E2-1712 has transits of 0.24% every 2.767 days. Ground-based photometry of E2-1712 was performed at the Wise Observatory on 28 December 2007. It was found that no nearby target undergoes eclipse, and the transit event detected by CoRoT is not seen either, with only 0.24% depth. It is thus inferred that the CoRoT transit occurs on the main target and the background eclipsing binary scenario is rejected. Then, the star was observed with HARPS on 27 February and 1 March 2008: the cross-correlation function is 18 km s^{-1} wide, showing a fast rotating star; the projected velocity is 13.4 km s^{-1} . The RV variations between both measurements at phases 0.72 and 0.17 is 60 m/s, but, due to the rotationally broadened spectral lines, individual errors are as large as 59 and 54 m/s, thus of the order of the observed variation. A possible variation of the stellar line profile is observed, which could indicate a diluted eclipsing binary. Also, a rough determination of stellar parameters from the HARPS spectra shows that the parent star is evolved, with $T_{\text{eff}} = 6700 \pm 100 \text{ K}$ and $\log g$ between 3.5 and 4.0. The most probable scenario is a triple system, yet we cannot firmly conclude on this case.

E1-4998/102821773

The candidate E1-4998 shows a 1.9% deep transit at period of 10.08 days. We obtained one HARPS measurement of the star on 21 January 2008 and a second point on 27 February 2008 (Table 15). The observed variation is of 23 km s^{-1} but not in phase with the CoRoT ephemeris, nor with twice the CoRoT period. We can suggest a binary at a different period superimposed on a planet-hosting star or another binary. The available data and the low brightness of the star do not allow us a more definite solution. No ground-based photometry has been performed on this target, so that a BEB is not excluded. So this case remains unsolved.

E2-1677/102874481

E2-1677 shows a single transit of 3% depth detected in the IRa01, featuring a system with a period longer than 33 days. One spectrum was obtained with SOPHIE on 22 December 2008. It shows a fast rotating star and the cross-correlation function is too noisy for high-precision RV measurements, especially with no constraint on the orbit's ephemeris. On the other hand, photometric colours indicate an F type star; the deep transit then is probably due to a stellar companion rather than of planetary origin, and it could obviously be a spatially resolved BEB in the CoRoT mask as well.

E1-4108/102779966

Finally, E1-4108 shows periodic 0.5% transits with a 7.366 day period. Ground-based photometric observations obtained with CFHT/Megacam on 10 March 2008 indicate that the transit occurs on the main CoRoT target. Three HARPS measurements were performed in February 2008, which show no significant RV variation at the level of 20 m/s (Table 17). A preliminary

Table 14. Status of transit candidate resolution following the analysis of complementary observations.

WinID	Depth	CoRoT P ^a	Nature	K	RV P
		%	[d]		[km s ⁻¹] [d]
E1-2046	1.17	50.2 ^b	SB2	>15	–
E2-3010	1.72	23.2	SB2	>17	–
E2-3854	0.136	1.14	SB2	43	–
E2-3856	2.05	16.56	SB1	60	–
E1-1158	1.36	10.53	SB1	25	–
E2-0203	3.43	5.168	SB1	16.9	–
E2-2430	1.16	3.587	SB1	23.5	–
E1-0399	1.5	33.06	SB1	20.5	–
E2-1736	1.18	21.72	SB1	15.5	–
E2-2604	0.25	3.82	aperture BEB	–	–
E2-1136	0.17	1.22	aperture BEB	–	–
E2-4300	0.51	5.806	aperture BEB	–	–
E1-0288	0.37	7.89	aperture BEB	–	–
E2-3425	0.36	1.185	aperture BEB	–	–
E2-1857	0.47	0.822	unresolved BEB	6.3	8.734
E2-2009	0.41	10.85	unresolved BEB	–	21.69
E1-2329	0.37	1.867	unresolved BEB	–	3.734
E1-3336	0.17	1.389	unresolved BEB	–	–
E2-0704	0.72	2.15	unresolved BEB	–	–
E1-4617	4.0	19.76	hot/fast star	–	–
E1-0783	0.64	>32	hot/fast star	–	–
E2-4467	1.4	16.45	hot/fast star	–	–
E1-4591	0.29	4.295	hot/fast star	–	–
E2-1677	3.0	>33	hot/fast star	–	–
E2-1712	0.24	2.767	unknown	–	–
E1-4998	1.9	10.08	unknown	>23	–
E1-4108	0.5	7.366	unknown	<0.02	–
E2-1126	2.16	1.509	planet	0.188	–
E1-0330	1.2	9.202	planet	0.063	–

^a for a more accurate determination of CoRoT period, see Paper I. ^b The period of this candidate was not measured during IRa01, but was inferred after it was re-observed by CoRoT during LRa01 at the end of 2008.

analysis of stellar fundamental parameters in these HARPS spectra shows that it is a cool main-sequence star (Table 2 and Deleuil et al., in prep.), with estimated mass and radius of $0.8 M_{\odot}$ and $0.8 R_{\odot}$. Such a faint star requires a large effort in spectroscopy for a complete confirmation, which has not been achieved so far. Preliminary information points towards a sub-Jovian planetary candidate (less than 3 times Neptune's mass and 1.6 times Neptune's radius), but for which no mass determination has yet been made. Alternatively, it could also be a triple system or diluted EB.

We are left with 8 cases for which no definite solution can be given. Most of them consist of fast rotators or early-type stars, for which no high-precision radial-velocity measurement is possible. E1-4108 is our only planetary candidate left, with a confirmation that the transit occurs on the main target and a main-sequence cool parent star. All the conclusions of our complementary observations, and their analysis, are given in Table 14.

3. Statistics

3.1. Stellar population

We used pre-launch observations (Deleuil et al. 2009) for a statistical estimate of the stellar population in IRa01. The classification method (Barbieri et al., in prep.) uses a comparison of magnitudes with reddened isochrones of stars of different types. The best-fit solution is extracted using Bayesian statistics. At small

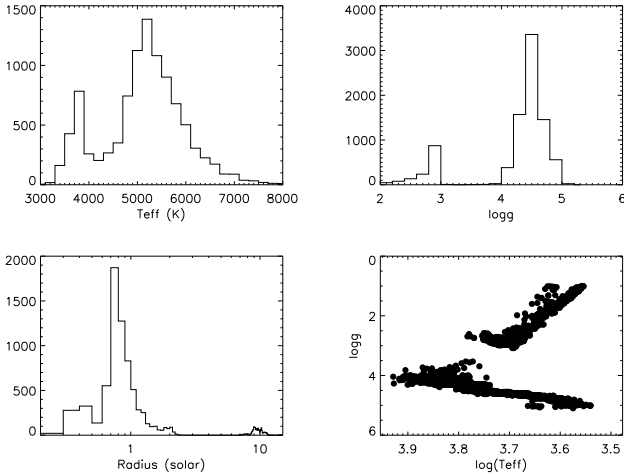


Fig. 8. The histograms of effective temperatures, $\log g$, first-order estimate of the stellar radius in the IRa01 target sample, and HR-diagram equivalent of this stellar field presented as $\log g$ versus effective temperature (*bottom right*).

latitudes above the Galactic plane, the CoRoT fields are characterised by an inhomogeneous interstellar content, which strongly affects identification of the evolutionary stage of a given target: a nearby red dwarf may be confused with a distant giant, or the opposite, as for candidates E2-2430 and E2-3854. The stellar radius may be strongly misestimated for certain classes of effective temperature, and thus the planet-likelihood ranking of a detected transit event must not rely only on a photometric analysis. It was thus decided for the follow-up campaign of IRa01, not to withdraw an event based on its being estimated as a giant.

The stellar field observed during the IRa01 is located at about RA = 06h47mn and Dec. = $-01^{\circ}51'$ or Galactic coordinates [214.0, -1.9]. The stellar population of IRa01 targets, after selection in the field, is composed of 9872 stars in the magnitude range $r = 11.25$ –16. Histograms of parameters issued from pre-launch photometry are shown in Fig. 8, as well as a temperature-luminosity diagram. The population of this target sample is dominated by the main sequence, which comprises up to 75% of the targets. According to our classification scheme, the mean radius is about $1 R_{\odot}$ and the mean effective temperature is below 6000 K. This is not to be compared directly with models of the Galaxy (Robin et al. 2004), since some selection criteria have been applied. The number of dwarf stars is overestimated by 25% in our target sample, compared to a simulation with the complete stellar field. This difference is due to a combination of 1) the selection of targets; 2) misclassification of giant stars; and 3) an ill-constrained reddening law in the Galaxy model towards this line of sight.

3.2. Discussion of statistics

We recall that 191 transiting candidates have been detected in IRa01, among which 141 are obvious eclipsing binaries, and 29 of the 50 planetary candidates were followed up for confirmation. The results of the present study in terms of transiting planet detection can be compared to expectations, both to assess the efficiency of the survey and to constrain the statistical properties of exoplanets. With only two planets detected in IRa01, however, a very detailed analysis is not warranted at this point. We give here our main conclusions on the topic, and refer further discussion to global analyses including more CoRoT fields.

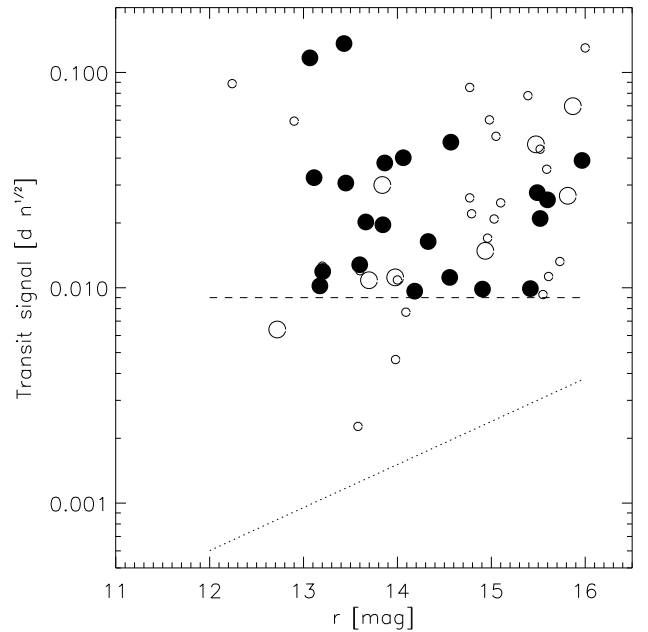


Fig. 9. Transit signal vs. magnitude for the planetary transit candidates discussed in this paper (large symbols). Closed symbols are objects confirmed as eclipsing binaries or transiting planets. Small symbols show the location of candidates of Paper I that were not followed up. The dashed line shows the threshold model, the dotted line shows the threshold based on ideal assumptions.

Transit detection threshold

We model the transit signal detection threshold as in Pont et al. (2006). That study shows that a threshold model as a signal-to-noise cutoff $\frac{d \cdot n^{1/2}}{\sigma^{1/2}} > S_T$ provided a good description for magnitude-limited photometric transit surveys included in this study as a function of magnitude and transit signal ($d \cdot n^{1/2} > 3$, σ is a characterisation of the noise over the transit timescale including systematic effects, and S_T the detection threshold). For ground-based surveys, values of $\sigma = 1$ – 3×10^{-3} are typical, but lower values are expected for space photometry.

Figure 9 shows the position of the candidates in the magnitude vs. transit signal ($d \cdot n^{1/2}$) plane. We use the lower envelope of the candidates confirmed by the follow-up as being genuine transiting planets or eclipsing binaries to estimate the effective detection threshold. Rather surprisingly, the threshold shows no dependence on magnitude. This is the case when correlated fluctuations (due either to instrumental effects or to real variability in the stellar flux) dominate the detection statistic compared to random noise. The dashed line shows a limit at $d \cdot n^{1/2} = 0.009$.

For comparison, the dotted line shows the “ideal” CoRoT detection limit, using photon-noise limited statistics and $S_T = 10$ (such as used for instance in the pre-launch estimates of Bordé et al. 2003). The detection threshold is substantially higher than in pre-launch models, especially for the bright targets. The detection was carried out with a preliminary reduction pipeline and detrending algorithms that have been improved since, so that it is possible that some low-SNR candidates can be recovered at the brightest magnitudes in the future. In Fig. 9, one may see that 4 transiting candidates lie between both lines of expected and actual detection thresholds (E1-0783 and 3 candidates from Paper I). They were not followed-up as single

transits or unpromising candidates, and are not considered further in discussing the threshold.

Hot Jupiters

Figure 9 shows that all transits with amplitude higher than $dn^{1/2} > 3 \times 10^{-3}$ are detectable. Consequently, all transiting hot Jupiters should be detected, since with transit depths near 10^{-2} and $n \gg 1$, they will clearly exceed this limit. Previous surveys have established that the frequency of transiting hot Jupiters in a magnitude-limited galactic population is of the order of 1 per 2000 main-sequence stars (Gaudi et al. 2005; Fressin et al. 2007). There are about 8000 dwarfs among the IRa01 targets, so that 4 transiting hot Jupiters are expected, weighing towards the fainter end of the survey.

In this instance, 2 hot Jupiters were detected, around targets in the brighter end of the sample. The difference between the expectations and what was observed is not significant in itself, but the tendency of the number of detections to be lower than expectations and always situated at the brighter end of the sample is confirmed in all CoRoT fields analysed so far. The first six planets revealed by CoRoT all have host stars in the bright half of the target range, on average about two per field.

We see three possible explanations for the dearth of hot Jupiters detected thus far in CoRoT fields: (1) There is a real lack of Jupiter-like planets at the faint end of the sample; (2) Transiting hot Jupiters around fainter targets were rejected when selecting candidates from the detection list; and (3) Transiting hot Jupiters are included in the sample, but were not confirmed by radial velocity.

At this point, all these explanations seem unlikely:

1. the colour-magnitude diagram of the target population does not show any population change between the bright and faint end of the target range;
2. hot Jupiter transits are easy to identify at the level of signal-to-noise afforded by the CoRoT data, and in this first Corot run, every effort was made to err on the side of caution when including candidates for follow-up;
3. the status of all but five planetary candidates (E1-4108, E1-4591, E1-4617, E2-4467 and E1-4998) was determined by complementary observations; we cannot conclude on the four last cases because their parent star has a rotationally broadened line profile.

Our best guess is that the reason is a combination of (2) and (3). The difficulty of identifying and confirming transiting planets in the CoRoT sample is a very steep function of magnitude. At the faintest end (as for E1-4617, E2-4467 and E1-4998), random noise and instrumental systematics can affect the detectability and apparent shape of the transit signal. On the radial-velocity side, the targets become too faint for follow-up with 1–2 m class telescopes (CORALIE and SOPHIE in our case), and require expensive 4–10-m class telescopes (HARPS in our case). Background eclipses also become much harder to rule out with ground-based photometry. It is probably not a coincidence that other surveys, such as TrES, also see their yields of hot Jupiter detections biased towards the bright end compared to statistical simulations.

Thus, when interpreting the present CoRoT results statistically, we warn that an effective cut at $R < 14$ may be needed in the detection/confirmation model, beyond which the actual characteristics of the detection/confirmation procedure are very difficult to model.

Small planets

Close-in planets in the mass range between Neptune and Saturn are known from radial-velocity surveys to be rarer than hot Jupiters around normal stars. Therefore, we expect a rate of detection of the order of unity or less per CoRoT field, even if the candidate census is complete. The lack of detection in IRa01 is obviously compatible with this estimate, and does not allow further conclusions.

Smaller planets may be more abundant. A detection threshold near $dn^{1/2} = 1.3 \times 10^{-2}$ corresponds for instance to a transit depth of 3×10^{-3} with $P = 3$ days, given the ~ 60 -day duration of the run. This is the signal of a $4.5-R_{\text{Earth}}$ planet across a solar-type star. Therefore, this set of candidates has a low sensitivity to planets smaller in size than Neptune. It could have been detected in IRa01 only on very close orbits or around small stars (which are rare in such a magnitude-limited sample).

4. Conclusion

Table 14 gives the state-of-the-art solution for all 29 IRa01 candidates for which follow-up observations are considered as complete. We unambiguously identify 1) two planets; 2) nine eclipsing and spectroscopic binaries; 3) five background eclipsing binaries located a few arcsec away from the main CoRoT target and included in the photometric mask; 4) five diluted eclipsing binaries or possible triple systems. The remaining candidates fall into two categories: 5) five candidates have a hot parent star for which no radial-velocity measurement is possible; and 6) three stars show no detectable radial-velocity variation over time. Over these eight unsolved cases, several have not been followed-up with ground-based photometry to check for a nearby background eclipsing binary, so this scenario cannot be excluded. Finally, a single candidate, E1-4108, is still a potential planetary system with confirmation feasible, although it would require a relatively large effort in gathering more data ($V = 15.4$ and RV semi-amplitude less than 20 m/s).

The lessons learned from the IRa01 follow-up operations can be summarized as follows: 1) time-critical ground-based photometry is a key step in the confirmation process, and unfortunately, the main bottleneck of these operations. Such observations must be done not too early (one-two months after the discovery), but not too late (typically less than 2 years) to obtain precise ephemeris values and definite conclusions. In some configurations, transits with a good visibility are extremely rare; a good coverage in longitude is essential; 2) For faint targets, both photometry and radial-velocity becomes very difficult. Although for IRa01, several targets with magnitudes higher than 15 were actually followed up with HARPS, and identified, this requires a large effort and the collected data is not always conclusive. This is, however, where most of giant transiting planets would lie.

In order to be more efficient in future fields observed by CoRoT, one would need a stronger confidence in the lightcurve analysis components, since four candidates have had a late detection of their faint secondary. With refined tools, the CoRoT team can now use this information in a systematic way. Then, a more intensive effort on ground-based photometry is necessary, and as soon as possible after the transit detection. The identification of early-type stars and fast rotators may help screening the candidate list, but does not help resolve the scenarios. Finally, high-precision radial-velocity measurements on faint targets ($V > 15$) is time consuming with HARPS and did not

show promising results for IRa01; such measurements were not given high priority for the follow-up operations, not allowing the confirmation of some giant planets.

References

- Aigrain, S., Collier Cameron, A., Ollivier, M., et al. 2008, *A&A*, 488, L43
Alonso, R., Alapini, A., Aigrain, S., et al. 2009, *A&A*, 506, 353
Barge, P., Baglin, A., Auvergne, M., et al. 2008, *A&A*, 482, L17
Bean, J. L. 2009, *A&A*, 506, 369
Bordé, P., Rouan, D., & Léger, A. 2003, *A&A*, 405, 1137
Bouchy, F., Moutou, C., & Queloz, D. 2009, *IAU Symp.*, 253, 129
Brown, T. M. 2003, *ApJ*, 593, L125
Carpano, S., Cabrera, J., Alonso, R., et al. 2009, *A&A*, 506, 491
Deleuil, M., Meunier, J.-C., Surace, C., et al. 2009, *AJ*, 138, 649
Fressin, F., Guillot, T., Morello, V., & Pont, F. 2007, *A&A*, 475, 729
Gaudi, B. S., Seager, S., & Mallen-Ornelas, G. 2005, *ApJ*, 623, 472
Gillon, M., Magain, P., Chantry, V., et al. 2007, in *Transiting Extrapolar Planets Workshop*, ed. C. Afonso, D. Weldrake, & T. Henning, *ASP Conf. Ser.*, 366, 113
Gillon, M., Demory, B.-O., Triaud, A. H. M. J., et al. 2009, *A&A*, 506, 359
Moutou, C., Bruntt, H., Guillot, T., et al. 2008, *A&A*, 488, L47
Pont, F., Zucker, S., & Queloz, D. 2006, *MNRAS*, 373, 231
Robin, A. C., Reylé, C., Derrière, S., & Picaud, S. 2004, *A&A*, 416, 157
Snellen, I. A. G., de Mooij, E. J. W., & Albrecht, S. 2009, *Nature*, 459, 543
Surace, C., Alonso, R., Barge, P., et al. 2008, in *SPIE Conf. Ser.*, 7019

Pages 331 to 336 (Tables 2 to 13, 15 to 17 and Figs. 4 to 7) are available in the electronic edition of the journal at
<http://www.aanda.org>

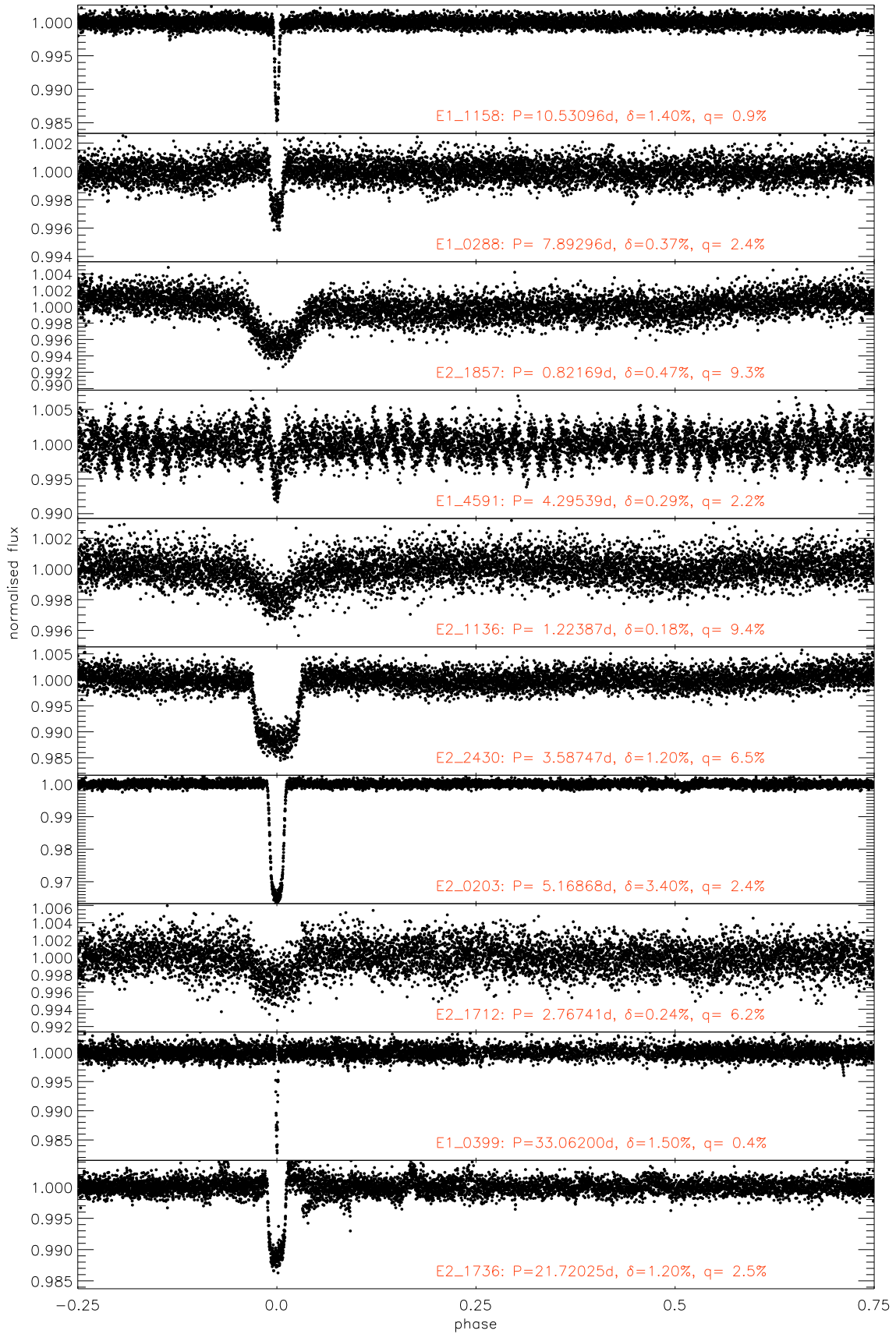


Fig. 4. CoRoT lightcurves of all candidates discussed in this paper: the light curve is phase-folded and the full orbital phase is shown. The iterative reconstruction filter (Alapini & Aigrain, *subm.*) is applied to the data, in order to correct for long-term instrumental and activity-related features while preserving the variation at the transit period.

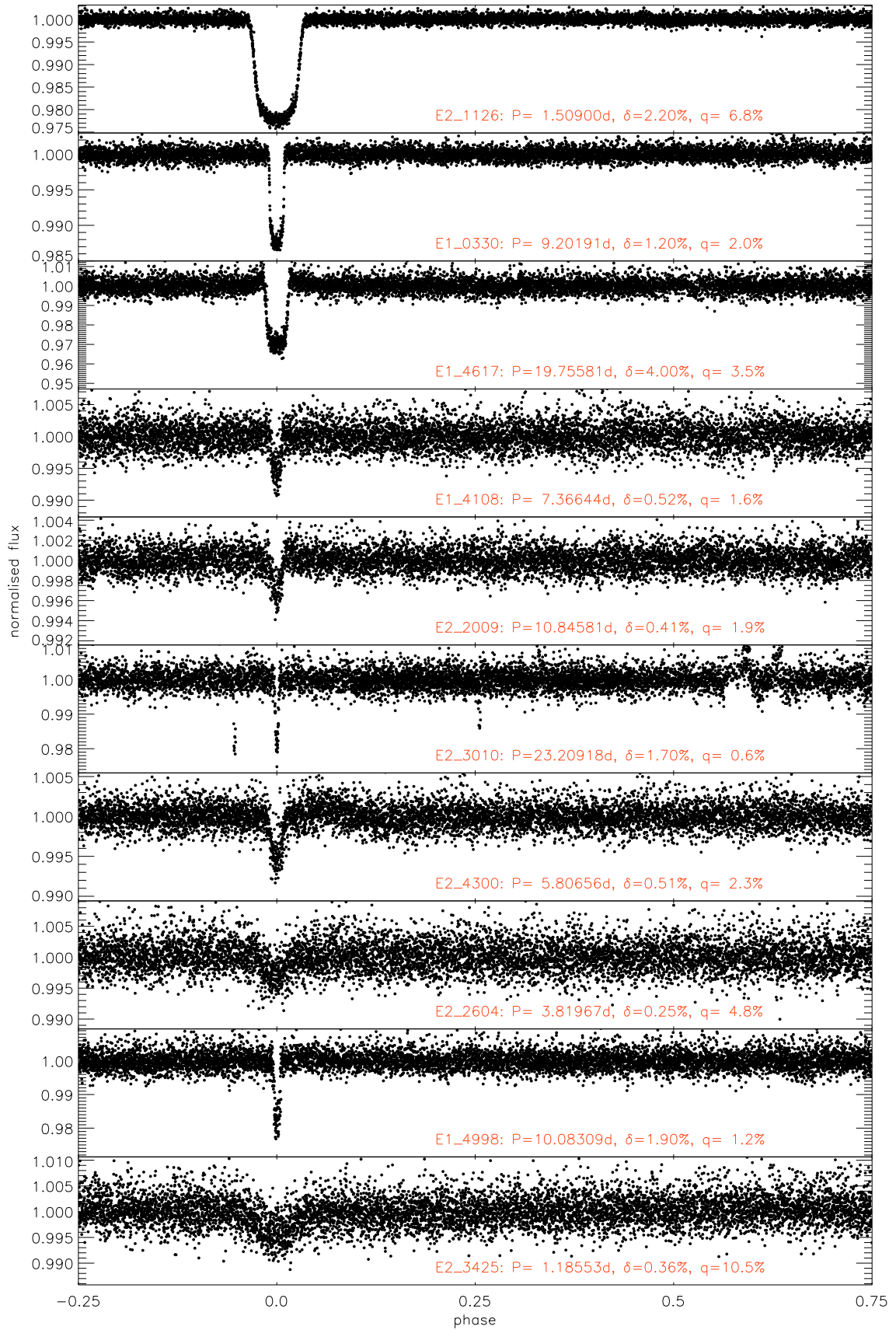


Fig. 5. CoRoT lightcurves of all candidates discussed in this paper (cont'd).

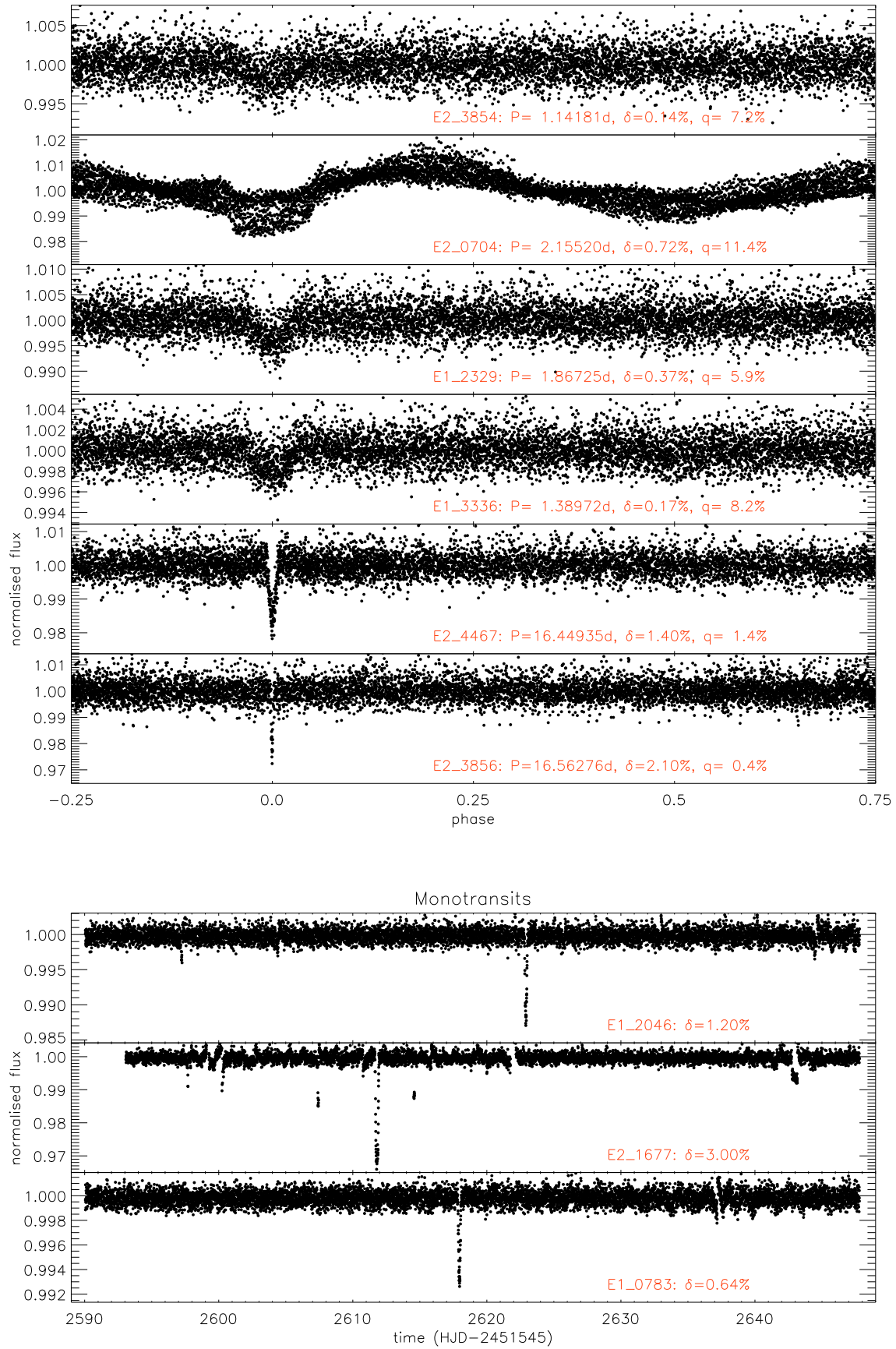


Fig. 6. CoRoT lightcurves of all candidates discussed in this paper (cont'd). For single transits, the full light curve is shown against Julian Date.

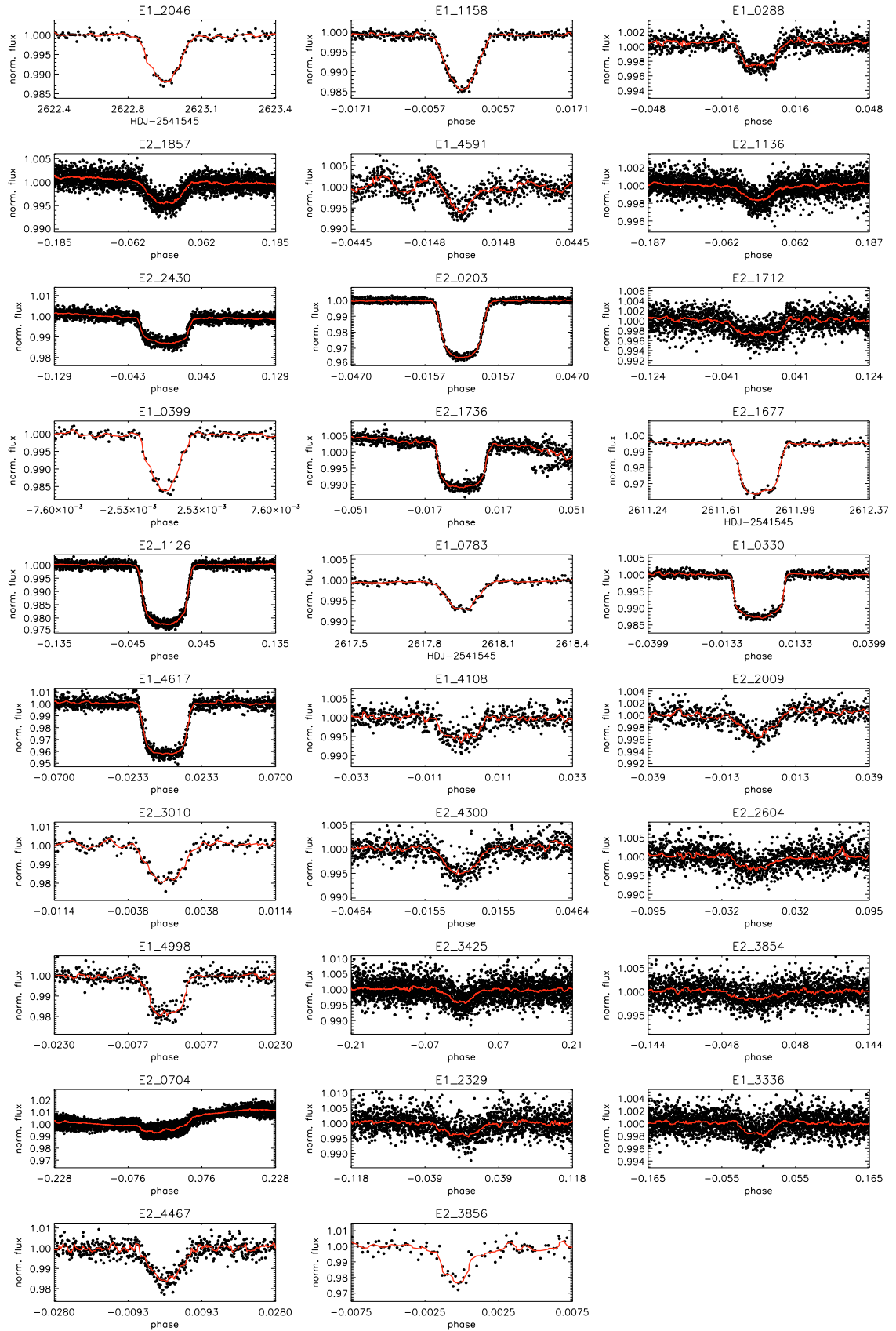


Fig. 7. CoRoT lightcurves of all candidates discussed in this paper (cont'd): zoom on the primary transits. The X-axis corresponds to the orbital phase when the period is determined, and Julian Date otherwise.

Table 2. Pre-launch information on IRa01 transit candidates derived from multi-colour photometry.

WinID	CoRoT ID	RA	Dec	B^a	V	r	J^b	K	SpT	Teff ^c	Instr.	Conta ^d
E1-2046	102723949	06:44:10.95	-01:11:13.24	14.885	13.958	13.598	12.355	11.683	K0III	5000	PH	0.0101
E2-3010	102800106	06:45:57.58	-02:28:00.73	16.82	15.883	15.489	13.896	13.363	K2V	4800	PH	0.046
E2-3854	102841669	06:47:09.41	-02:46:39.11	16.419	15.333	14.906	12.919	12.383	K5III	4500	PH	0.038
E2-3856	102954464	06:49:37.33	-02:30:49.14	17.548	16.478	15.966	14.304	13.540	K5V	4500	PH	0.010
E1-1158	102763847	06:45:05.23	-01:21:25.24	13.604	13.199	13.112	12.530	12.374	F0V	7250	PH	0.004
E2-0203	102825481	06:46:43.20	-02:35:58.31	14.025	13.308	13.068	12.058	11.681	G1V	5800	PH	0.000
E2-2430	102815260	06:46:25.78	-03:09:13.28	15.74	14.893	14.569	13.122	12.648	F2V	7000	SO	0.019
E1-0399	102829121	06:46:49.37	-01:23:11.62	14.708	13.933	13.663	12.543	12.126	G4V	5550	PH	0.003
E2-1736	102855534	06:47:30.58	-02:55:04.12	14.681	14.062	13.845	12.762	12.412	G0V	5900	PH	0.086
E2-2604	102805893	06:46:08.99	-02:02:00.35	16.513	15.703	15.416	14.110	13.635	G8V	5200	PH	0.0194
E2-1136	102809071	06:46:15.36	-03:05:19.61	13.497	13.228	13.204	12.611	12.496	A9V	7400	PH	0.08
E2-4300	102802430	06:46:02.21	-02:00:13.43	15.234	14.552	14.327	13.135	12.817	G3V	5600	PH	0.212
E1-0288	102787048	06:45:36.24	-00:43:17.40	14.149	13.452	13.174	12.269	11.928	F9V	6000	PH	0.17
E2-1857	102798247	06:45:53.90	-02:47:15.90	14.857	14.259	14.062	13.050	12.674	F9V	5950	PH	0.006
E2-2009	102788073	06:45:37.69	-01:58:09.30	16.48	14.865	14.184	11.542	10.614	M0II	3800	PH	0.039
E1-2329	102869286	06:47:49.45	-00:36:29.05	16.895	15.957	15.520	14.327	13.715	G9IV	5100	PH	0.062
E1-3336	102876631	06:48:00.16	-01:05:05.96	16.417	15.099	14.557	12.479	11.651	K8V	4050	PH	0.016
E1-4617	102753331	06:44:50.87	-00:42:53.28	16.855	16.158	15.868	14.563	14.087	G7V	5300	PH	0.002
E1-0783	102895957	06:48:26.40	-01:14:31.34	13.246	12.852	12.720	11.951	11.760	F2IV	6800	PH	0.028
E2-4467	102940315	06:49:20.63	-02:05:37.72	17.079	16.177	15.814	14.033	13.570	K2III	4800	PH	0.000
E1-4591	102806520	06:46:10.25	-01:42:23.70	14.452	13.863	13.697	12.705	12.418	F9V	6000	PH	0.315
E2-1712	102826302	06:46:44.59	-03:02:32.21	14.868	14.197	13.976	12.843	12.530	F5IV	6700	HA	0.04
E2-3425	102835817	06:47:00.12	-02:34:07.14	16.671	15.903	15.598	14.320	13.862	G7III	5800	HA	0.26
E1-4998	102821773	06:46:36.92	-01:06:15.77	16.41	15.71	15.475	14.354	13.909	G2V	5700	PH	0.258
E2-0704	102855472	06:47:30.49	-02:36:40.14	15.085	14.215	13.865	12.514	12.028	G7III	5400	HA	0.102
E2-1677	102874481	06:47:57.12	-02:56:10.89	14.403	13.941	13.839	12.989	12.707	F4V	6500	PH	0.015
E1-4108	102779966	06:45:26.87	-01:14:09.46	16.512	15.412	14.936	13.571	12.880	K2V	5100	HA	0.0437
E2-1126	102890318	06:48:19.20	-03:06:07.77	14.197	13.624	13.431	12.462	12.149	G0V	5950	UV	0.0383
E1-0330	102912369	06:48:46.70	-00:40:21.97	14.312	13.694	13.450	12.619	12.288	F0V	6190	UV	0.003

^a Optical magnitudes were measured at the Isaac Newton Telescope with the Wide Field Camera; B and V filters are from the Harris system, and r from the Sloan system. ^b J and K magnitudes are 2MASS measurements. ^c The origin of the estimate for effective temperature (Teff), spectral type and luminosity class (SpT) may be from spectral analysis (HA for HARPS, UV for UVES, SO for SOPHIE) or by default, from multicolour photometry. ^d “conta” is the ratio between the background flux and the total flux.

Table 3. Radial-velocity measurements of E2-3854. SO stands for SOPHIE and HA for HARPS.

JD-2 400 000.	ϕ	RV1 [km s ⁻¹]	RV2 [km s ⁻¹]	σ [km s ⁻¹]	Instr.
54494.416	0.36	1.56	98.35	0.2	SO
54505.364	0.95	80.8	12.55	0.5	SO

Table 4. Radial-velocity measurements of 0102763847/E1-1158.

JD-2 400 000.	ϕ	RV [km s ⁻¹]	σ [km s ⁻¹]	Instr.
54 521.328	0.21	-17.795	0.070	SO
54 526.291	0.69	28.152	0.080	SO

Table 5. Radial-velocity measurements of E1-0399. CO stands for CORALIE at the Euler 120cm Swiss telescope.

JD-2 400 000.	ϕ	RV [km s ⁻¹]	σ [km s ⁻¹]	Instr.
54 477.734	0.86	43.05	0.08	CO
54 495.566	0.39	15.43	0.11	CO

Table 6. Radial-velocity measurements of E2-3856.

JD-2 400 000.	ϕ	RV [km s ⁻¹]	σ [km s ⁻¹]	Instr.
54 530.641	0.24	4.74	0.02	SO
54 549.546	0.39	26.19	0.02	SO

Table 7. Radial-velocity measurements of E2-2430.

JD-2 400 000.	ϕ	RV [km s ⁻¹]	σ [km s ⁻¹]	Instr.
54 502.409	0.23	51.36	0.111	SO
54 504.401	0.79	97.25	0.098	SO

Table 8. Radial-velocity measurements of 0102855534/E1-1736.

JD-2 400 000.	ϕ	RV [km s ⁻¹]	σ [km s ⁻¹]	Instr.
54 497.471	0.29	27.07	0.121	SO
54 507.424	0.75	57.55	0.099	SO

Table 9. Radial-velocity measurements of 0102855472/E2-0704.

JD-2 400 000.	ϕ CoRoT	RV [km s ⁻¹]	σ [km s ⁻¹]	Instr.
54 526.599	0.78	39.36	0.031	HA
54 527.611	0.24	39.32	0.032	HA

Table 10. Radial-velocity measurements of 0102798247/E2-1857.

JD-2 400 000.	ϕ CoRoT	ϕ RV	RV [km s ⁻¹]	σ [km s ⁻¹]	Instr.
54 499.329	0.353	0.437	16.35757	0.0724	SO
54 501.369	0.836	0.670	25.33129	0.0546	SO
54 514.361	0.647	0.158	16.97243	0.0681	SO
54 515.306	0.797	0.266	14.94759	0.0634	SO
54 518.399	0.561	0.620	23.51338	0.0403	SO
54 525.281	0.937	0.408	15.583	0.064	SO
54 527.305	0.400	0.640	22.97	0.05	SO
54 528.326	0.643	0.757	27.058	0.050	SO
54 548.542	0.246	0.072	20.746	0.070	HA
54 549.506	0.419	0.182	16.310	0.079	HA
54 550.540	0.678	0.300	14.424	0.111	HA
54 551.549	0.905	0.416	16.000	0.055	HA

Table 11. Radial-velocity measurements of 0102788073/E2-2009.

JD-2 400 000.	ϕ CoRoT	ϕ 2P	RV [km s ⁻¹]	σ [km s ⁻¹]	Instr.
54 503.426	0.344	0.672	79.90	0.054	SO
54 519.398	0.817	0.408	80.00	0.025	SO
54 527.351	0.550	0.775	79.95	0.058	SO
54 528.365	0.644	0.822	79.96	0.041	SO
54 540.348	0.749	0.374	79.83	0.040	SO
54 545.346	0.209	0.605	79.87	0.020	SO
54 546.329	0.300	0.650	79.36	0.030	SO
54 548.501	0.50	0.75	79.94 (F0)	0.047	HA
54 548.501	0.50	0.75	80.078 (G2)	0.047	HA
54 548.501	0.50	0.75	80.131 (K5)	0.047	HA
54 551.515	0.77	0.89	79.987 (F0)	0.035	HA
54 551.515	0.77	0.89	79.928 (G2)	0.035	HA
54 551.515	0.77	0.89	79.915 (K5)	0.035	HA

Table 12. Radial-velocity measurements of 0102869286/E1-2329.

JD-2 400 000.	ϕ CoRoT	ϕ 2P	RV [km s ⁻¹]	σ [km s ⁻¹]	Instr.
54 519.638	0.693	0.847	15.786	0.02	HA
54 522.609	0.284	0.642	15.822	0.017	HA
54 525.556	0.863	0.431	15.743	0.014	HA

Table 13. Radial-velocity measurements of 0102876631/E1-3336.

JD-2 400 000.	ϕ	RV [km s ⁻¹]	σ [km s ⁻¹]	Instr.
54 497.425	0.163	71.425	0.036	SO
54 502.360	0.715	71.583	0.033	SO
54 503.376	0.446	71.466	0.047	SO
54 517.626	0.700	71.62 (F0)	0.021	HA
		71.595 (G2)		
		71.606 (K5)		
54 519.547	0.082	71.397 (F0)	0.019	HA
		71.463 (G2)		
		71.492 (K5)		
54 522.552	0.245	71.478 (F0)	0.011	HA
		71.524 (G2)		
		71.546 (K5)		

Table 15. Radial-velocity measurements of E1-4998.

JD-2 400 000.	ϕ	RV [km s ⁻¹]	σ [km s ⁻¹]	Instr.
54 487.645	0.24	25.	0.2	HA
54 524.625	0.91	3.	0.4	HA

Table 16. Radial-velocity measurements of E2-3425.

JD-2 400 000.	ϕ	RV [km s ⁻¹]	σ [km s ⁻¹]	Instr.
54 744.875	0.74	27.6847	0.028	HA
54 746.863	0.41	27.7201	0.036	HA

Table 17. Radial-velocity measurements of E1-4108.

JD-2 400 000.	ϕ	RV [km s ⁻¹]	σ [km s ⁻¹]	Instr.
54 516.602	0.39	99.15	0.015	HA
54 518.645	0.66	99.14	0.019	HA
54 519.592	0.80	99.15	0.018	HA